Arch Appl Mech (2016) 86:1913–1926
DOI 10.1007/s00419-016-1149-1

REPLY

Anna Jablonka

Stochastic sensitivity analysis for structural dynamics systems via the second-order perturbation

Received: 6 October 2015 / Accepted: 11 May 2016 / Published online: 27 June 2016

Abstract The problem of dynamic structural response dependent on random variations of design parameters is presented in the paper. A variational formulation of the FEM equations of motion and the probability distribution of time instant stochastic sensitivity are described. The suggested perturbation technique is completely second-order accurate, unlike in conventional approach. For instance, three different structural systems, excited by a Heaviside impact, are implemented and discussed. Numerical results for the first two probabilistic moments of displacement sensitivity gradients are obtained by the mode superposition method. Concluding remarks show that dynamic sensitivity analysis in the stochastic context better describes the real structural response and allows us to find the appropriate design point.

Keywords Stochastic · Dynamic sensitivity · Finite element · Completely second-order accuracy

1 Introduction

Nowadays, buildings are often characterized by complicated forms and slenderness. Therefore, an appropriate computational technique, such as the finite element method (FEM), which is implemented in most structural analysis computer codes [1–3] is needed. Since designers are required to make the optimal use of building materials, structures must inevitably be lightweight and strong, and this is exactly why design sensitivity analysis [4,5] may be necessary. Sensitivity analysis can be carried out with respect to global [6,7] or local design variables [8–12]. Global design variables are, e.g., the overall geometry, overall shape and topology. Local design variables, such as cross-sectional area, element thickness, Young modulus, Poisson's ratio, yield stress, mass and loading, are considered in this paper. Besides static design sensitivity, dynamic sensitivity is worth analyzing especially for structures exposed to wind or sea waves.

Uncertainty of design variables is included so far in building standards by empirical safety factors. For more complex or less typical cases, however, standardized recommendations may not be sufficient. Making a stochastic analysis is thus essential. It can be carried out by the spectral approach [13] or by the perturbational approach [14–19], where all the functions of random variables are expanded exponentially. The stochastic and sensitive formulations can be considered jointly for the same or different design variables, [18–21].

In the conventional perturbational approach, by using the first two probabilistic moments for random variables on input, the first two probabilistic moments of the structural response are obtained on output, wherein only the expectations are with second-order accuracy, and the cross-covariances are with first-order accuracy [18,19]. In this paper, a modified version of these perturbation schemes for dynamic sensitivity is presented, in which both probabilistic moments on output are second-order accurate, as for the static sensitivity given in [22].

A. Jablonka (✉)
Structure Theory Department, West Pomeranian University of Technology, Al. Piastow 50, 70-311 Szczecin, Poland
E-mail: ajablonka@zut.edu.pl

After the introduction, in the second section the equations of motion are obtained in the context of FEM. The third section describes the stochastic dynamic sensitivity for a time instant. In the next section, numerical results of stochastic dynamic sensitivity analysis are shown for three different structural systems, with truss, shell and beam elements. Summary remarks finish the paper.

2 Finite element model of dynamics

The variational Hamilton's principle states that the real displacement field, among all permissible, satisfying boundary and initial conditions at times t_1, t_2 in the volume Ω, makes stationary the functional of the total energy. The total energy is the sum of kinetic energy T, potential energy V and external forces work W, leading to

$$\delta \int_{t_1}^{t_2} (T - V)\mathrm{d}t + \delta \int_{t_1}^{t_2} W \mathrm{d}t = 0 \tag{1}$$

with

$$T = \int_{\Omega} \frac{1}{2}\, \rho\, \dot{\mathbf{u}}^{\mathrm{T}} \dot{\mathbf{u}}\, \mathrm{d}\Omega \tag{2}$$

$$V = \int_{\Omega} \frac{1}{2}\quad ^{\mathrm{T}}\quad \mathrm{d}\Omega \tag{3}$$

$$W = \int_{\partial\Omega} \widehat{\mathbf{t}}^{\mathrm{T}} \mathbf{u}\, \mathrm{d}(\partial\Omega) \tag{4}$$

where ρ is the mass density, and $= \{\varepsilon_{11}, \varepsilon_{22}, \varepsilon_{33}, \sqrt{2}\varepsilon_{12}, \sqrt{2}\varepsilon_{13}, \sqrt{2}\varepsilon_{23}\}$, $\mathbf{u} = \{u_i\}$, $\dot{\mathbf{u}} = \{\dot{u}_i\}$, $= \{\sigma_{11}, \sigma_{22}, \sigma_{22}, \sqrt{2}\sigma_{12}, \sqrt{2}\sigma_{13}, \sqrt{2}\sigma_{23}\}$ and $\widehat{\mathbf{t}} = \{\widehat{t_i}\}$, $i = 1, 2, 3$, are the strain, displacement, velocity, stress and the boundary force vectors, respectively. By the engineering character of the paper, in Eq. (4) the body forces are neglected.

As a result of the transformation described in [23,24], the FEM equation system of motion is obtained as

$$\mathbf{M}\,\ddot{\mathbf{q}} + \mathbf{C}\,\dot{\mathbf{q}} + \mathbf{K}\,\mathbf{q} = \mathbf{Q} \tag{5}$$

where $\mathbf{M} = [M_{\alpha\beta}]$, $\mathbf{C} = [C_{\alpha\beta}]$ and $\mathbf{K} = [K_{\alpha\beta}]$, $\mathbf{q} = \{q_\alpha\}$, $\dot{\mathbf{q}} = \{\dot{q}_\alpha\}$, $\ddot{\mathbf{q}} = \{\ddot{q}_\alpha\}$ and $\mathbf{Q} = \{Q_\alpha\}$, $\alpha = 1, 2, \ldots, N$, are the mass, damping and stiffness matrices, nodal displacement, velocity, acceleration and load vectors, respectively, with N being the system number of degrees of freedom. The explicit forms of the stiffness and nodal load matrices for specific types of the finite elements can be found in [1–3], for instance.

For the sake of presentation transparency, the indicial notation will be used from now on. Equations (5) are rewritten in the residual form, where twice repeated indices implying summation as

$$Q_\alpha - K_{\alpha\beta}\, q_\beta - C_{\alpha\beta}\, \dot{q}_\beta - M_{\alpha\beta}\, \ddot{q}_\beta = 0 \tag{6}$$

3 Time instant stochastic sensitivity

For the multi-degree-of-freedom (MDOF) system, at the time instant $\tau = t$, the structural response can be defined by the function

$$\Phi = G \int_0^t [q_\alpha(\mathbf{h}, \mathbf{b}; \tau), \mathbf{h}]\, \delta(t - \tau)\mathrm{d}\tau, \qquad t \in [0, T] \tag{7}$$

where t denotes the running terminal time and $\delta(t-\tau)$ is the Dirac delta distribution. The function (7) is satisfying the equations of motion (5) and being an explicit and implicit function of the vector of design variables $\mathbf{h} = \{h^d\}$, $d = 1, 2, \ldots, D$, and the vector of random variables $\mathbf{b} = \{b^r\}$, $r = 1, 2, \ldots, R$, i.e.,

$$
\begin{aligned}
&Q_\alpha(\mathbf{h}, \mathbf{b}; \tau) - K_{\alpha\beta}(\mathbf{h}, \mathbf{b})\, q_\beta(\mathbf{h}, \mathbf{b}; \tau) - C_{\alpha\beta}(\mathbf{h}, \mathbf{b})\, \dot{q}_\beta(\mathbf{h}, \mathbf{b}; \tau)\\
&\quad - M_{\alpha\beta}(\mathbf{h}, \mathbf{b})\, \ddot{q}_\beta(\mathbf{h}, \mathbf{b}; \tau) = 0, \qquad \alpha, \beta = 1, 2, \ldots, N\\
&q_\alpha(\mathbf{h}, \mathbf{b}; 0) = 0, \quad \dot{q}_\alpha(\mathbf{h}, \mathbf{b}; 0) = 0
\end{aligned} \tag{8}
$$

The first two probabilistic moments—expectations $\overline{b}^{\,r}$ and cross-covariances $\mathrm{Cov}(b^r, b^s)$ of the random variables b^r are defined as

$$
\overline{b}^{\,r} = \mathrm{E}\left[b^r\right] = \int_{-\infty}^{+\infty} b^r\, p\,(b^r)\mathrm{d}b^r \tag{9}
$$

$$
\mathrm{Cov}(b^r, b^s) = \mathrm{E}\left[(b^r - b_0^r)(b^s - b_0^s)\right] = \mathrm{R}(b^r, b^s)\sqrt{\mathrm{Var}(b^r)\mathrm{Var}(b^s)} \tag{10}
$$

with

$$
\mathrm{R}\,(b^r, b^s) = \int_{-\infty}^{+\infty}\int_{-\infty}^{+\infty} b^r b^s\, p(b^r, b^s)\mathrm{d}b^r \mathrm{d}b^s \tag{11}
$$

$$
\mathrm{Var} = \alpha^2 \mathrm{E}^2\left[b^r\right] \tag{12}
$$

where $\mathrm{R}(b^r, b^s)$, $\mathrm{Var}(b^r, b^s)$, $p(b^r, b^s)$ and α denote functions of correlation, variance, joint probability density and the coefficient of variation, respectively.

The functions of random variables $K_{\alpha\beta}$, $C_{\alpha\beta}$, $M_{\alpha\beta}$, q_α and Q_α will be handled by the perturbation scheme. Assume that $K_{\alpha\beta}$, $C_{\alpha\beta}$, $M_{\alpha\beta}$, q_β and Q_α are twice differentiable with respect to the design variables h^d and the random variables b^r. Using the chain rule of differentiation, and since the running terminal time t takes on some a priori selected value in the time interval $[0, T]$, leads to the expression for the derivative of Φ with respect to h^d in the form

$$
\begin{aligned}
\Phi^{;d}(t) &= \int_0^t \left[G^{,d}(\tau)\,\delta(t-\tau) + G_{,\alpha}(\tau)\, q_\alpha^{;d}(\tau)\,\delta(t-\tau)\right]\mathrm{d}\tau\\
&= G^{,d}(t) + \int_0^t G_{,\alpha}(\tau)\, q_\alpha^{;d}(\tau)\,\delta(t-\tau)\mathrm{d}\tau
\end{aligned} \tag{13}
$$

where $(\cdot)^{;d}$ is the first ordinary derivative with respect to the dth design variable, $(\cdot)^{,d}$ and $(\cdot)_{,\alpha}$ are the first partial derivatives with respect to the dth design variable and αth nodal displacement, respectively. The components $G^{,d}$ and $G_{,\alpha}$ in Eq. (13) are known, because G is an explicit function of its arguments. While q_α are implicit with respect to h_d, the derivatives $q_\alpha^{;d}$ must be determined. Differentiating the equation of motion (8) with respect to the design variables h_d yields

$$
M_{\alpha\beta}\ddot{q}_\beta^{;d}(\tau) + C_{\alpha\beta}\dot{q}_\beta^{;d}(\tau) + K_{\alpha\beta}q_\beta^{;d}(\tau) - R_\alpha^d(\tau) = 0 \tag{14}
$$

where

$$
R_\alpha^d(\tau) = Q_\alpha^{,d}(\tau) - M_{\alpha\beta}^{,d}\ddot{q}_\beta(\tau) - C_{\alpha\beta}^{,d}\dot{q}_\beta(\tau) - K_{\alpha\beta}^{,d}q_\beta(\tau) \tag{15}
$$

To eliminate $q_\alpha^{;d}$ from (13), the adjoint system method is employed. Pre-multiplying (14) by the transpose of an adjoint vector $\lambda_\alpha(\tau)$, which is initially independent of random design variables, integrating by parts with respect to τ and equating the coefficients at $q_\alpha^{;d}$ in the resulting equation and (13), we obtain the differential equations of motion for the adjoint system in the form

$$
\begin{aligned}
&M_{\alpha\beta}\ddot{\lambda}_\beta(\tau) - C_{\alpha\beta}\dot{\lambda}_\beta(\tau) + K_{\alpha\beta}\lambda_\beta(\tau) = G_{,\alpha}(t)\,\delta(t-\tau)\\
&\lambda_\alpha(t) = 0, \quad \dot{\lambda}_\alpha(t) = 0, \quad \tau \in [0, t], \qquad t \in [0, T]
\end{aligned} \tag{16}
$$

Substituting (16) into (13) and taking into account (14) we obtain

$$
\Phi^{;d}(t) = G^{,d}(t) + \int_0^t \lambda_\alpha(\tau)\, R_\alpha^d(\tau)\,\mathrm{d}(\tau) \tag{17}
$$

Now, the functions of random variables $M_{\alpha\beta}$, $C_{\alpha\beta}$, $K_{\alpha\beta}$, Q_α, $G_{.\alpha}$, q_β, λ_α, $M_{\alpha\beta}^{.d}$, $C_{\alpha\beta}^{.d}$, $K_{\alpha\beta}^{.d}$, $Q_\alpha^{.d}$ and $G^{.d}$ are expanded around the expectations $\overline{b}^{\,r}$ via the second-order perturbation, with a small parameter θ, generally expressed as

$$(\cdot)(\mathbf{h},\mathbf{b}) = (\cdot)^0 + \theta(\cdot)^{;r}\Delta b^r + \frac{1}{2}\,\theta^2(\cdot)^{;rs}\Delta b^r\Delta b^s, \qquad r,s = 1,2,\ldots,R \tag{18}$$

where Δb^r is the perturbational increment of b^r with respect to b_0^r, and $(\cdot)^0$, $(\cdot)^{;r}$ and $(\cdot)^{;rs}$ describe the zeroth, first and second ordinary derivatives with respect to b^r.

The expansions of $M_{\alpha\beta}$, $C_{\alpha\beta}$, $K_{\alpha\beta}$, Q_α, $G_{.\alpha}$, q_β and λ_α are substituted into (8) and (16). Equating the coefficients of the given parameter θ to zeroth, first and second power leads to

– 1 pair of the zero-order equations

$$\begin{aligned}
&M_{\alpha\beta}^0\ddot{q}_\beta^0(\tau) + C_{\alpha\beta}^0\dot{q}_\beta^0(\tau) + K_{\alpha\beta}^0 q_\beta^0(\tau) = Q_\alpha^0(\tau)\\
&q_\alpha^0(0) = 0; \quad \dot{q}_\alpha^0(0) = 0; \quad \tau\in[0,t]; \quad t\in[0,T]\\
&M_{\alpha\beta}^0\ddot{\lambda}_\beta^0(\tau) - C_{\alpha\beta}^0\dot{\lambda}_\beta^0(\tau) + K_{\alpha\beta}^0\lambda_\beta^0(\tau) = G_{.\alpha}^0(t)\delta(t-\tau)\\
&\lambda_\alpha^0(t) = 0; \quad \dot{\lambda}_\alpha^0(t) = 0; \quad \tau\in[0,t]; \quad t\in[0,T]
\end{aligned} \tag{19}$$

– r pairs of the first-order equations

$$\begin{aligned}
&M_{\alpha\beta}^0\ddot{q}_\beta^{;r}(\tau) + C_{\alpha\beta}^0\dot{q}_\beta^{;r}(\tau) + K_{\alpha\beta}^0 q_\beta^{;r}(\tau) = Q_\alpha^r(\tau)\\
&q_\alpha^{;r}(0) = 0; \quad \dot{q}_\alpha^{;r}(0) = 0; \quad \tau\in[0,t]; \quad t\in[0,T]\\
&M_{\alpha\beta}^0\ddot{\lambda}_\beta^{;r}(\tau) - C_{\alpha\beta}^0\dot{\lambda}_\beta^{;r}(\tau) + K_{\alpha\beta}^0\lambda_\beta^{;r}(\tau) = G_\alpha^r(\tau,t)\\
&\lambda_\alpha^{;r}(t) = 0; \quad \dot{\lambda}_\alpha^{;r}(t) = 0; \quad \tau\in[0,t]; \quad t\in[0,T]\\
&r = 1,2,\ldots,R
\end{aligned} \tag{20}$$

– 1 pair of the second-order equations

$$\begin{aligned}
&M_{\alpha\beta}^0\ddot{q}_\beta^{(2)}(\tau) + C_{\alpha\beta}^0\dot{q}_\beta^{(2)}(\tau) + K_{\alpha\beta}^0 q_\beta^{(2)}(\tau) = Q_\alpha^{(2)}(\tau)\\
&q_\alpha^{(2)}(0) = 0; \quad \dot{q}_\alpha^{(2)}(0) = 0; \quad \tau\in[0,t]; \quad t\in[0,T]\\
&M_{\alpha\beta}^0\ddot{\lambda}_\beta^{(2)}(\tau) - C_{\alpha\beta}^0\dot{\lambda}_\beta^{(2)}(\tau) + K_{\alpha\beta}^0\lambda_\beta^{(2)}(\tau) = G_\alpha^{(2)}(\tau,t)\\
&\lambda_\alpha^{(2)}(t) = 0; \quad \dot{\lambda}_\alpha^{(2)}(t) = 0; \quad \tau\in[0,t]; \quad t\in[0,T]
\end{aligned} \tag{21}$$

where

$$\begin{aligned}
q_\alpha^{(2)} &= \tfrac{1}{2}\,q_\alpha^{;rs}\,\mathrm{Cov}(b^r,b^s)\\
\lambda_\alpha^{(2)} &= \tfrac{1}{2}\,\lambda_\alpha^{;rs}\,\mathrm{Cov}(b^r,b^s)
\end{aligned}, \qquad r,s = 1,2,\ldots,R \tag{22}$$

while the first- and second-order primary and adjoint generalized load vectors are defined by

$$\begin{aligned}
Q_\alpha^r(\tau) &= Q_\alpha^{;r}(\tau) - M_{\alpha\beta}^{;r}\ddot{q}_\beta^0(\tau) - C_{\alpha\beta}^{;r}\dot{q}_\beta^0(\tau) - K_{\alpha\beta}^{;r}q_\beta^0(\tau)\\
G_\alpha^r(\tau,t) &= G_{.\alpha}^{;r}(t)\delta(t-\tau) - M_{\alpha\beta}^{;r}\ddot{\lambda}_\beta^0(\tau) + C_{\alpha\beta}^{;r}\dot{\lambda}_\beta^0(\tau) - K_{\alpha\beta}^{;r}\lambda_\beta^0(\tau)
\end{aligned} \tag{23}$$

$$\begin{aligned}
Q_\alpha^{(2)}(\tau) &= \Big[\frac{1}{2}\,Q_\alpha^{;rs}(\tau) - M_{\alpha\beta}^{;r}\ddot{q}_\beta^{;s}(\tau) - C_{\alpha\beta}^{;r}\dot{q}_\beta^{;s}(\tau) - K_{\alpha\beta}^{;r}q_\beta^{;s}(\tau)\\
&\quad -\frac{1}{2}\,M_{\alpha\beta}^{;rs}\ddot{q}_\beta^0(\tau) - \frac{1}{2}\,C_{\alpha\beta}^{;rs}\dot{q}_\beta^0(\tau) - \frac{1}{2}\,K_{\alpha\beta}^{;rs}q_\beta^0(\tau)\Big]\mathrm{Cov}(b^r,b^s)\\
G_\alpha^{(2)}(\tau,t) &= \Big[\frac{1}{2}\,G_{.\alpha}^{;rs}(t)\delta(t-\tau) - M_{\alpha\beta}^{;r}\ddot{\lambda}_\beta^{;s}(\tau) + C_{\alpha\beta}^{;r}\dot{\lambda}_\beta^{;s}(\tau) - K_{\alpha\beta}^{;r}\lambda_\beta^{;s}(\tau)\\
&\quad -\frac{1}{2}\,M_{\alpha\beta}^{;rs}\ddot{\lambda}_\beta^0(\tau) + \frac{1}{2}\,C_{\alpha\beta}^{;rs}\dot{\lambda}_\beta^0(\tau) - \frac{1}{2}\,K_{\alpha\beta}^{;rs}\lambda_\beta^0(\tau)\Big]\mathrm{Cov}(b^r,b^s)
\end{aligned} \tag{24}$$

Having solved the initial-terminal systems (19)–(21) for the zero-, first- and second-order primary and adjoint displacements, velocities and accelerations, the solution to the time instant stochastic sensitivity problem can be received by setting $\theta = 1$ in the expansions of $M_{\alpha\beta}, C_{\alpha\beta}, K_{\alpha\beta}, Q_\alpha, G_{.\alpha}, q_\beta, \dot{q}_\beta, \ddot{q}_\beta, \lambda_\alpha, \dot{\lambda}_\alpha$ and $\ddot{\lambda}_\alpha$ via the second-order perturbation. In this way, the dynamic case of the second-order accurate expectations and cross-covariances for the time instant sensitivity gradient are written, respectively, as

$$\begin{aligned}
\mathrm{E}\left[\Phi^{\cdot d}(t)\right] &= G^{0.d}(t) + \int_0^t \left\{\mathcal{A}_\alpha^d(\tau)\left[\lambda_\alpha^0(\tau) + \lambda_\alpha^{(2)}(\tau)\right] - \mathcal{D}_\alpha^{d(2)}(\tau)\lambda_\alpha^0(\tau)\right\}\mathrm{d}\tau \\
&\quad + \left\{\frac{1}{2}G^{\cdot d;rs}(t) + \int_0^t \left[\mathcal{B}_\alpha^{dr}(\tau)\lambda_\alpha^{;s}(\tau) + \mathcal{C}_\alpha^{drs}(\tau)\lambda_\alpha^0(\tau)\right]\mathrm{d}\tau\right\}\mathrm{Cov}(b^r, b^s) \qquad (25)
\end{aligned}$$

$$\begin{aligned}
\mathrm{Cov}(\Phi^{\cdot d}(t_1), \Phi^{\cdot e}(t_2)) &= \Bigg(G^{\cdot d;r}(t_1)G^{\cdot e;s}(t_2) \\
&\quad + G^{\cdot d;r}(t_1)\int_0^{t_2}\left[\mathcal{A}_\alpha^e(\tau)\lambda_\alpha^{;s}(\tau) + \mathcal{B}_\alpha^{es}(\tau)\lambda_\alpha^0(\tau)\right]\mathrm{d}\tau \\
&\quad + G^{\cdot e;r}(t_2)\int_0^{t_1}\left[\mathcal{A}_\alpha^d(\tau)\lambda_\alpha^{;s}(\tau) + \mathcal{B}_\alpha^{ds}(\tau)\lambda_\alpha^0(\tau)\right]\mathrm{d}\tau \\
&\quad + \int_0^{t_1}\int_0^{t_2}\Big\{\mathcal{A}_\alpha^d(\tau)\mathcal{A}_\beta^e(\nu)\lambda_\alpha^{;r}(\tau)\lambda_\beta^{;s}(\nu) \\
&\quad + \left[\mathcal{A}_\alpha^d(\tau)\mathcal{B}_\beta^{er}(\nu) + \mathcal{A}_\beta^e(\nu)\mathcal{B}_\alpha^{dr}(\tau)\right]\lambda_\alpha^{;s}(\tau)\lambda_\beta^0(\nu) \\
&\quad + \mathcal{B}_\alpha^{dr}(\tau)\mathcal{B}_\beta^{es}(\nu)\lambda_\alpha^0(\tau)\lambda_\beta^0(\nu)\Big\}\mathrm{d}\tau\,\mathrm{d}\nu \\
&\quad - \overline{\Phi}^{\cdot d}(t_1)\Bigg\{\frac{1}{2}G^{\cdot e;rs}(t_2) + \int_0^{t_2}\Big[\mathcal{B}_\alpha^{er}(\tau)\lambda_\alpha^{;s}(\tau) \\
&\quad + \mathcal{C}_\alpha^{ers}(\tau)\lambda_\alpha^0(\tau)\Big]\mathrm{d}\tau\Bigg\} - \overline{\Phi}^{\cdot e}(t_2)\Bigg\{\frac{1}{2}G^{\cdot d;rs}(\tau) \\
&\quad + \int_0^{t_1}\left[\mathcal{B}_\alpha^{dr}(\tau)\lambda_\alpha^{;s}(\tau) + \mathcal{C}_\alpha^{drs}(\tau)\lambda_\alpha^0(\tau)\right]\mathrm{d}\tau\Bigg\}\Bigg)\mathrm{Cov}(b^r, b^s) \\
&\quad + \overline{\Phi}^{\cdot d}(t_1)\int_0^{t_2}\left[\mathcal{D}_\alpha^{e(2)}(\tau)\lambda_\alpha^0(\tau) - \mathcal{A}_\alpha^e(\tau)\lambda_\alpha^{(2)}(\tau)\right]\mathrm{d}\tau \\
&\quad + \overline{\Phi}^{\cdot e}(t_2)\int_0^{t_1}\left[\mathcal{D}_\alpha^{d(2)}(\tau)\lambda_\alpha^0(\tau) - \mathcal{A}_\alpha^d(\tau)\lambda_\alpha^{(2)}(\tau)\right]\mathrm{d}\tau \qquad (26)
\end{aligned}$$

where

$$\begin{aligned}
\mathcal{A}_\alpha^d(\tau) &= Q_\alpha^{0.d}(\tau) - K_{\alpha\beta}^{0.d}q_\beta^0(\tau) - C_{\alpha\beta}^{0.d}\dot{q}_\beta^0(\tau) - M_{\alpha\beta}^{0.d}\ddot{q}_\beta^0(\tau) \\
\mathcal{B}_\alpha^{dr}(\tau) &= Q_\alpha^{\cdot d;r}(\tau) - K_{\alpha\beta}^{0.d}q_\beta^{;r}(\tau) - K_{\alpha\beta}^{\cdot d;r}q_\beta^0(\tau) - C_{\alpha\beta}^{0.d}\dot{q}_\beta^{;r}(\tau) \\
&\quad - C_{\alpha\beta}^{\cdot d;r}(\tau)\dot{q}_\beta^0(\tau) - M_{\alpha\beta}^{0.d}\ddot{q}_\beta^{;r}(\tau) - M_{\alpha\beta}^{\cdot d;r}\ddot{q}_\beta^0(\tau) \\
\mathcal{C}_\alpha^{drs}(\tau) &= \frac{1}{2}Q_\alpha^{\cdot d;rs}(\tau) - K_{\alpha\beta}^{\cdot d;r}q_\beta^{;s}(\tau) - \frac{1}{2}K_{\alpha\beta}^{\cdot d;rs}q_\beta^0(\tau) - C_{\alpha\beta}^{\cdot d;r}\dot{q}_\beta^{;s}(\tau) \\
&\quad - \frac{1}{2}C_{\alpha\beta}^{\cdot d;rs}\dot{q}_\beta^0(\tau) - M_{\alpha\beta}^{\cdot d;r}\ddot{q}_\beta^{;s}(\tau) - \frac{1}{2}M_{\alpha\beta}^{\cdot d;rs}\ddot{q}_\beta^0(\tau) \\
\mathcal{D}_\alpha^{d(2)}(\tau) &= K_{\alpha\beta}^{0.d}q_\beta^{(2)}(\tau) + C_{\alpha\beta}^{0.d}\dot{q}_\beta^{(2)}(\tau) + M_{\alpha\beta}^{0.d}\ddot{q}_\beta^{(2)}(\tau) \qquad (27)
\end{aligned}$$

with $t, t_1, t_2 \in [0, T]$; $d, e = 1, 2, \ldots, D$; $r, s = 1, 2, \ldots, R$; $\alpha, \beta = 1, 2, \ldots, N$.

It should be noted that the obtained cross-covariance matrix (26) is second-order accurate, and not the first-order one as in [18].

4 Numerical results

For illustration purposes, the dynamic sensitivity of displacement to random change of design parameters for three different structural systems is considered. First, the example of simple structure is considered for comparison the first- and second-order accuracy for the cross-covariance matrix. Next, the example known from [18] and discussed earlier for static sensitivity in [22] is analyzed. The numerical results given below are completely second-order accurate for the expectation vector and cross-covariance matrix, other than in [18]. Random design variables are defined by the thicknesses of shell elements and the cross-sectional areas of beam elements. Expectations and standard deviations, being the square root of variances, of dynamic sensitivity are presented in the graphs below. The stochastic sensitivity analysis is implemented by using a modified version of the computer code POLSAP, [25].

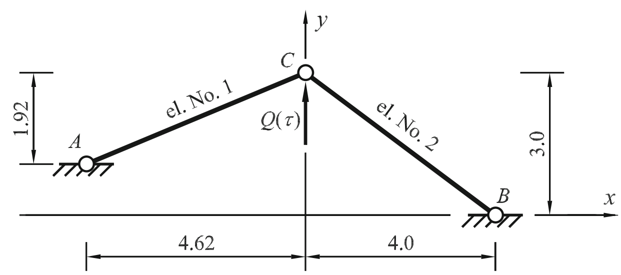

Fig. 1 Truss structure—FEM model

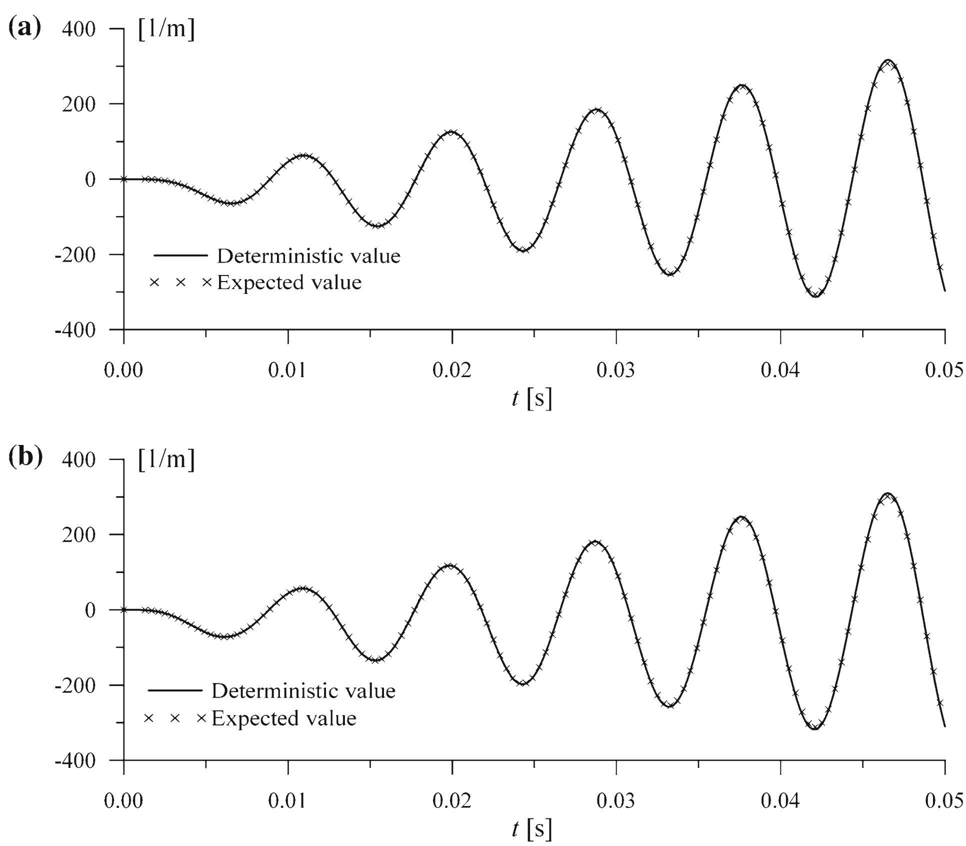

Fig. 2 Dynamic displacement sensitivity of: **a** element No. 1, **b** element No. 2—cross-sectional areas as a random design variables

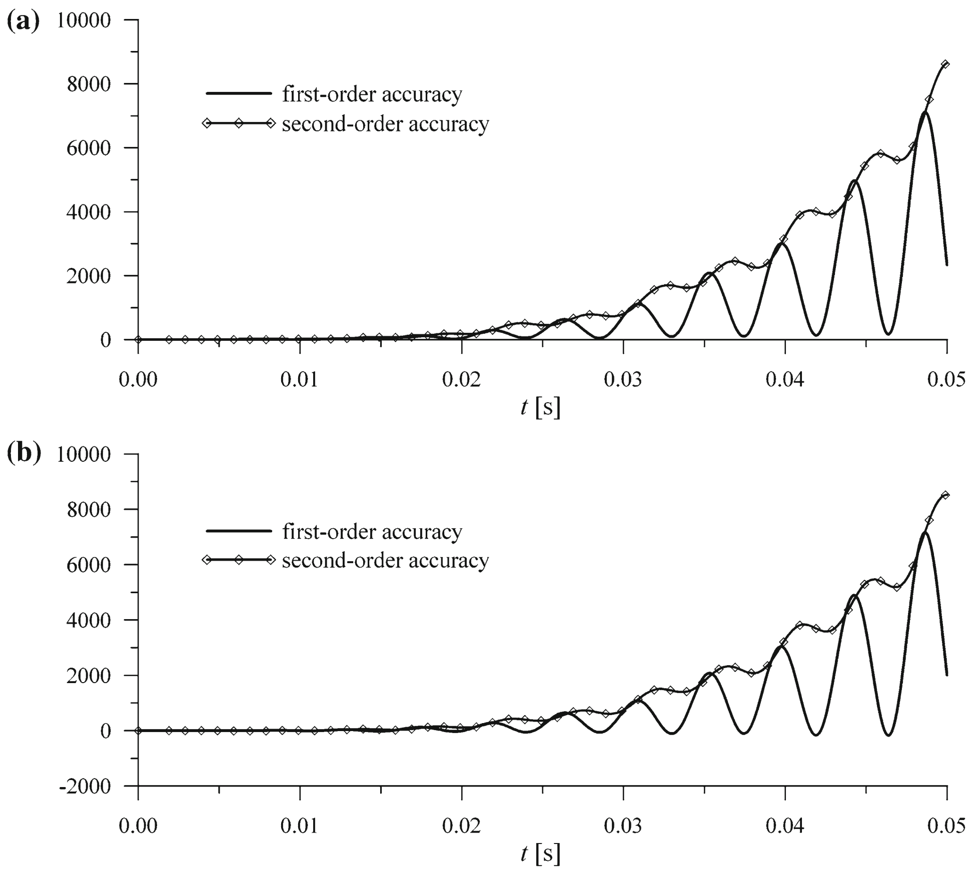

Fig. 3 Cross-covariances for dynamic displacement sensitivity of: **a** element No. 1, **b** elements No. 1 and No. 2

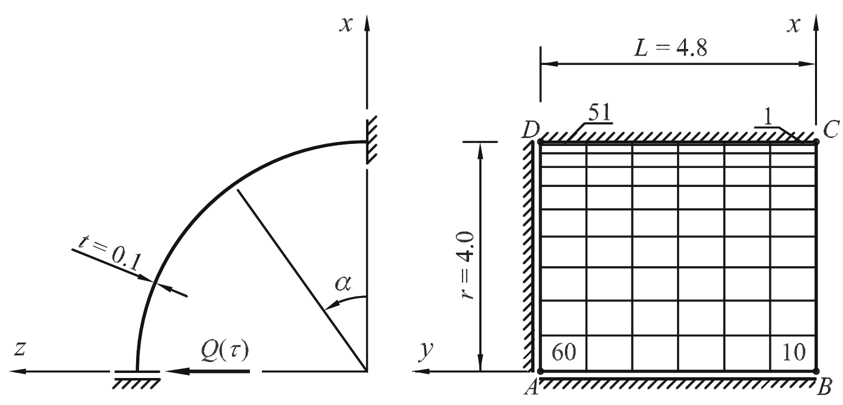

Fig. 4 Cylindrical shell—FEM model

4.1 Example 1: Two-element truss structure

The first example is only academic and is intended to show the difference between the first- and second-order accurate cross-covariances of dynamic displacement sensitivity. The structure consisting of two truss elements with a length $L = 5\,\mathrm{m}$ was analyzed, Fig. 1. The nodes A and B are locked on moving. The elements are designed with material characterized by Young's modulus $e = 200\,\mathrm{GPa}$ and density $\rho = 7.85\,\mathrm{g/cm^3}$. Random design variables are defined as cross-sectional areas a^r, $r = 1, 2$, with the means $a_0^r = \mathrm{E}\left[a^r\right] = 5 \times 10^{-3}\,\mathrm{m}^2$. The correlation function is of the form

Table 1 Shell: eigenproblem—numerical results

Vibration form	1	2	3	4	5	6	7	8	…
Frequency f (Hz)	2.38	7.49	11.19	15.40	16.96	22.12	24.63	25.73	…

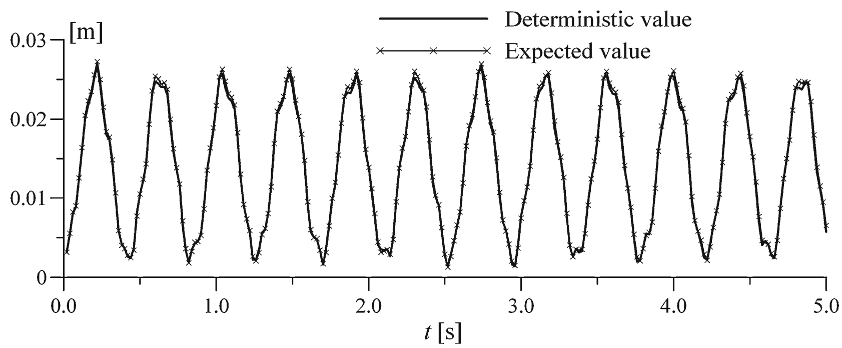

Fig. 5 Displacements at the node A

$$\mathrm{R}(a^r, a^s) = \exp\left(\frac{-|x^r - x^s|}{\lambda}\right) \exp\left(\frac{-|y^r - y^s|}{\lambda}\right) \tag{28}$$

where $\lambda = 0.5$ and the coefficient of variation $\alpha = 0.02$ are applied. The truss is loaded at the point C by the constant force $Q(\tau) = 1000\,\mathrm{kN}$, Fig. 1. The response function is described as

$$\Phi = \frac{|q|}{q_{\mathrm{all}}} - 1 < 0 \tag{29}$$

where the allowable vertical displacement $q_{\mathrm{all}} = 0.05$ at the node C is assumed.

A dynamic stochastic sensitivity analysis was carried out by the mode superposition technique using the program MATHEMATICA, [26]. The periods for the first and second vibration forms were: $T_1 = 8.87 \times 10^{-3}$ s, $T_2 = 5.07 \times 10^{-3}$ s. Maximum vertical displacements at the node C were approx. 0.02 m.

The expectations of displacement sensitivity of the node C to the change of cross-sectional areas were differed by 4 % from deterministic values, Fig. 2. The results of variance for dynamic displacement sensitivity of element No. 1 and cross-covariance for sensitivity of elements No. 1 and No. 2 are shown in Fig. 3. The calculations were done with first- and second-order accuracy. The covariances obtained with second-order accuracy are characterized by more constant increase in the time than covariances with first-order accuracy.

4.2 Example 2: Cylindrical thin shell structure

In Example 2, the time distributions of the sensitivity gradient for a thin shell structure, which is a quarter of a cylinder of radius $R = 4.0$ m and length $L = 4.8$ m, are considered, Fig. 4. The following boundary conditions are adopted: along the bound AB the x-displacements, and y- and z-rotations are zero, BC is entirely free, CD is fixed, along the bound DA the y-displacements, and x- and z-rotations are zero. The material is characterized by Young's modulus $e = 10$ GPa and Poisson's ratio $\nu = 0.3$. The finite element mesh of the shell consists of 60 equally rectangular elements. The shell thicknesses t^r, $r = 1, 2, \ldots, 60$, are random design variables with the means $t_0^r = \mathrm{E}\left[t^r\right] = 0.1$ m. The correlation function is described as

$$\mathrm{R}(t^r, t^s) = \exp\left(\frac{-|x^r - x^s|}{R\,\lambda}\right) \exp\left(\frac{-|y^r - y^s|}{L\,\lambda}\right) \tag{30}$$

where $\lambda = 0.25$ and the coefficient of variation $\alpha = 0.08$. The shell is loaded by constant force $Q(\tau) = 10\,\mathrm{kN}$ at the point A, Fig. 4, as a Heaviside step function, on the time interval $T = 5$ s divided into 2500 equal steps.

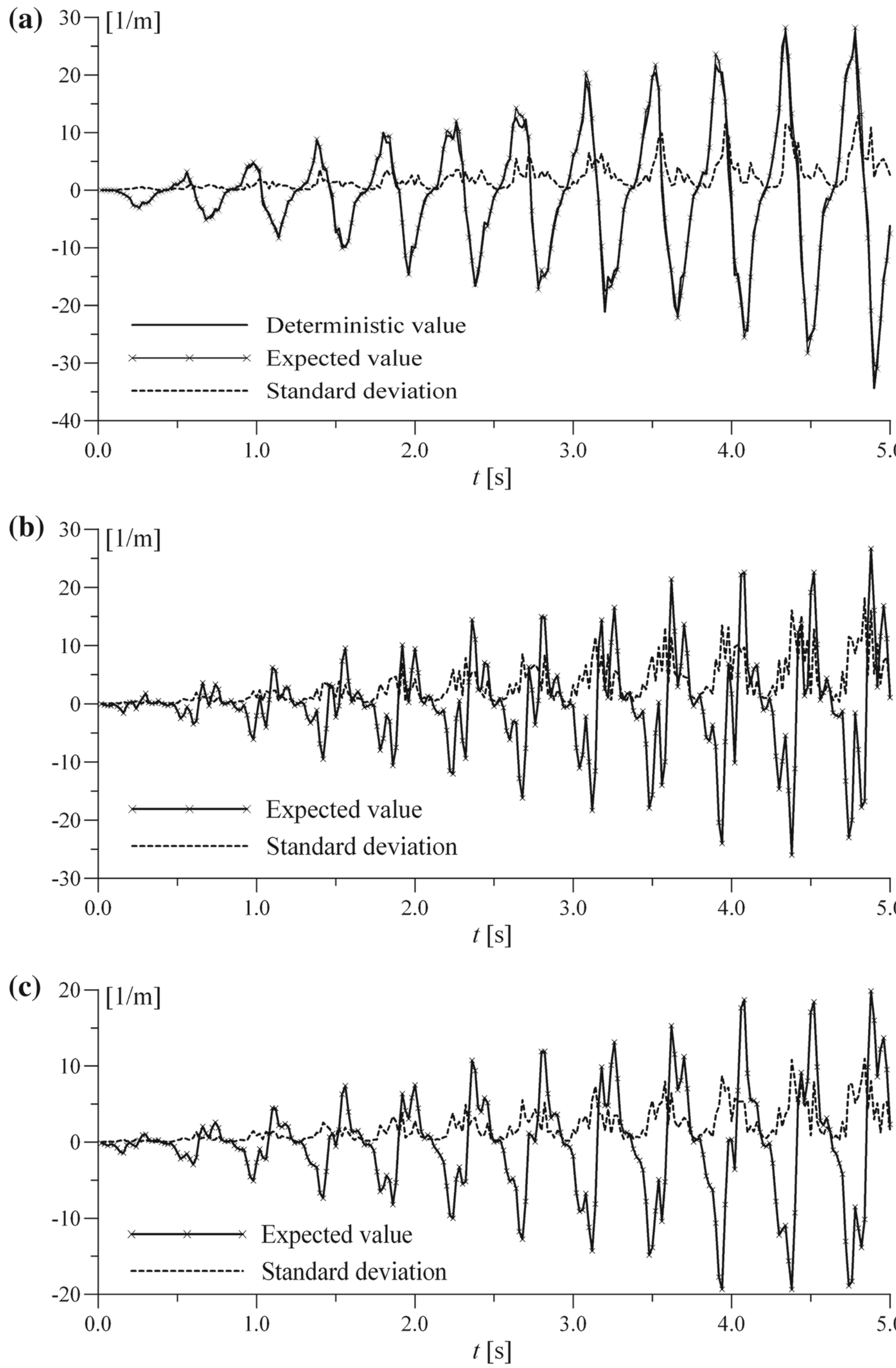

Fig. 6 Dynamic displacement sensitivity of: **a** el. No. 1, **b** el. No. 40, **c** el. No. 60—shell thicknesses as a random design variables

The response function takes the form

$$\Phi = \frac{1}{t}\int_0^t \int_\Omega \delta(x - x^*)\, q^2(x,\tau)\, \mathrm{d}\Omega\, \mathrm{d}\tau, \quad t \in [0, T] \tag{31}$$

where δ is the Dirac delta function and Ω is the structure volume. The terminal conditions of the adjoint system are $\lambda(t) = 0,\ \dot{\lambda}(t) = 0$. We assume that the allowable displacement q_z at the node A is 0.03.

A dynamic sensitivity analysis was carried out using the mode superposition technique with 10 lowest eigensystems. First, solving eigenproblem, eigenvalues and eigenvectors were received. The frequency for

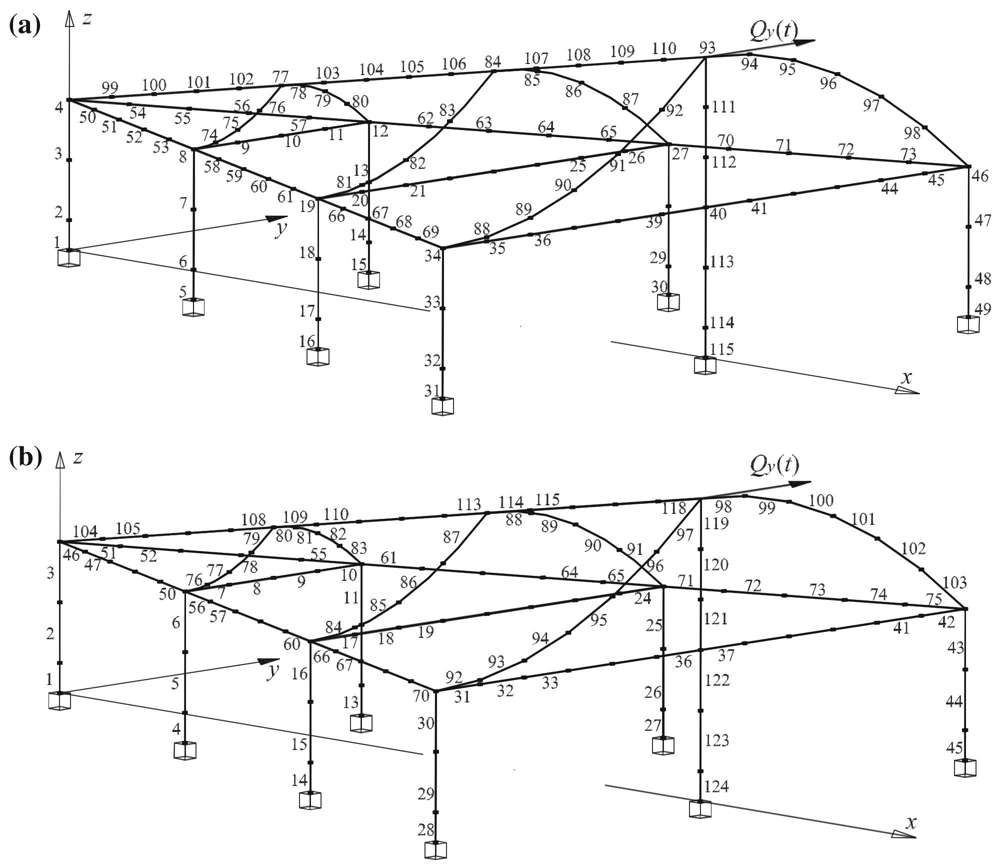

Fig. 7 Frame structure: **a** nodes of FEM model, **b** beam elements

Table 2 Frame: eigenproblem—numerical results

Vibration form	1	2	3	4	5	6	7	8	…
Frequency f (Hz)	2.84	2.91	3.31	3.80	4.57	4.72	4.76	5.42	…

the first form of vibration was 2.38 Hz, Table 1. The 60 correlated random variables were transformed into uncorrelated variables using 10 highest modes in the calculation.

The maximum displacements at the node A did not exceed 0.03 m, Fig. 5. The differences between the expected and deterministic values were about 2 %. The numerical results of displacement sensitivity of the node A to the change of element thicknesses for selected elements are shown in Fig. 6. The most sensitive results were obtained with the shell element No. 1 being around node C. The standard deviation of displacement sensitivity was about 30 % of the expectations.

4.3 Example 3: Frame structure

Example 3 concerns the time displacement response of a frame structure of length $L_x = 30$ m, maximum width $L_y^{\max} = 24$ m, minimum height $H_z^{\min} = 5$ m and maximum height $H_z^{\max} = 10$ m, Fig. 7. The structure was modeled with a FEM mesh with 124 beam elements. As for boundary conditions, nodes 1, 5, 15, 16, 30, 31, 49 and 115 are fixed. All the elements are designed with steel profiles characterized by Young's modulus $e = 210$ GPa and Poisson's ratio $\nu = 0.3$. Random design variables are defined as cross-sectional areas a^r, with expectations $a_0^r = \mathrm{E}\left[a^r\right] = 7.49 \times 10^{-3}\,\mathrm{m}^2$. Moments of torsion and inertia are considered as a measure of the cross-sectional areas squared, with $I_x = 1.594\, a^2$ and $I_y = I_z = 0.797\, a^2$. The correlation function is described as

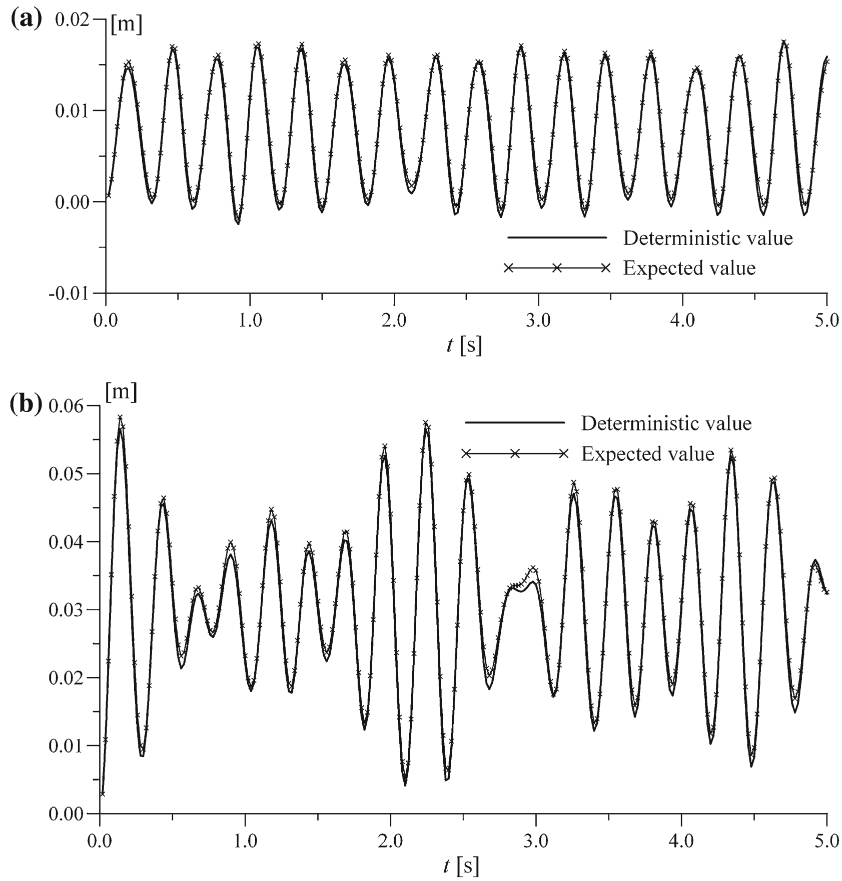

Fig. 8 Displacements: **a** q_x at the node 69, **b** q_y at the node 97

$$\mathrm{R}(a^r, a^s) = \exp\left(\frac{-|x^r - x^s|}{\lambda}\right) \exp\left(\frac{-|y^r - y^s|}{\lambda}\right) \exp\left(\frac{-|z^r - z^s|}{\lambda}\right) \tag{32}$$

where $\lambda = 0.1$ and the coefficient of variation $\alpha = 0.7$ are adopted. The response function takes also the form (31). The system is loaded at the point 93 by the constant force $Q_y(\tau) = 50\,\text{kN}$, Fig. 7, as a Heaviside function, on the time interval $T = 5\,\text{s}$ divided into 2500 steps. The allowable displacement $q_y = 0.3$ at the node 93 is assumed.

A sensitivity analysis is also conducted using the mode superposition technique with 10 lowest eigensystems. The frequency values for the first eight forms of vibration were presented in Table 2. It can be seen that the differences between the following values are small. A set of 124 correlated random variables was converted to a set of uncorrelated variables using 10 highest modes in the calculation.

The obtained displacements did not exceed the allowable limits. The results of displacements q_x at the node 69 and q_y at the node 97 are shown in Fig. 8. The expected and deterministic values differ by about 3 %.

Figures 9 and 10 give the expectations and standard deviations of dynamic displacement sensitivity of the node 93 to the change of cross-sectional areas of some elements. Elements No. 1, 27, 124 are distinguished by great sensitivity values. Some graphs, e.g., for element No. 114, are quite regular, others, e.g., for elements No. 1, 27, 41, 124, have varying amplitudes. The waveform for element No. 1, Fig. 9a), is characteristic for systems with beat phenomenon. The standard deviations of displacement sensitivity with respect to the beam cross-sectional areas were about 30–40 % of the expectations.

The numerical results of dynamic sensitivity analysis of the shell, Fig. 6, and of the frame, Figs. 9, 10, show that the time-dependent sensitivities gain positive values periodically in time, except Fig. 9c). The graph of sensitivity for element No. 1, Fig. 9a), particularly shows that positive values are higher than negative ones. The fact suggests that to decrease displacements at the considered points, decreasing the thickness of shell elements or the cross-sectional areas of beam elements may be appropriate. Such a proposition was already discussed in terms of statics by Jablonka and Hien [22].

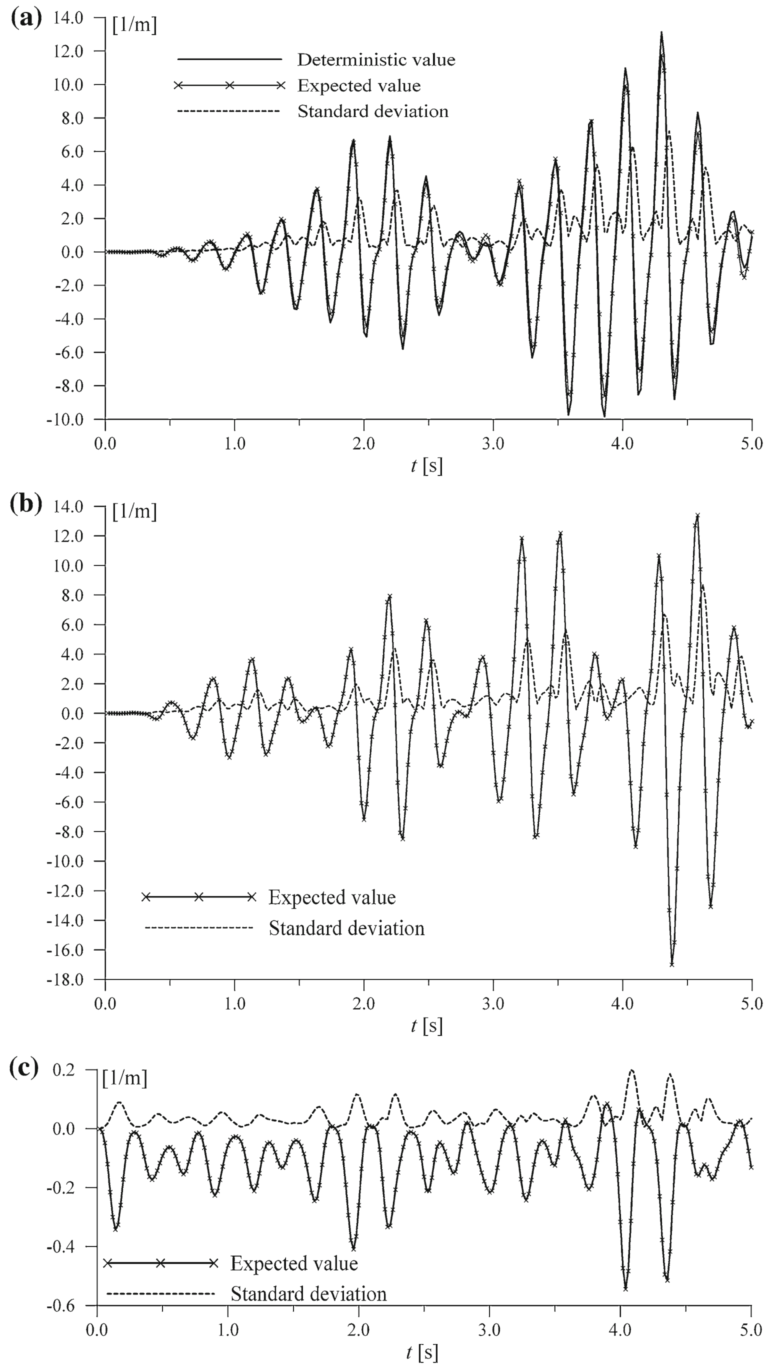

Fig. 9 Dynamic displacement sensitivity of: **a** el. No. 1, **b** el. No. 27, **c** el. No. 41—cross-sectional areas as a random design variables

5 Concluding remarks

A modified perturbation scheme for stochastic systems in a dynamic context, described in this paper, leads to completely second-order accurate both the probabilistic moments of time instant sensitivity. In a traditional perturbation scheme, only the expectations with second-order accuracy and first-order accurate cross-covariances were formulated.

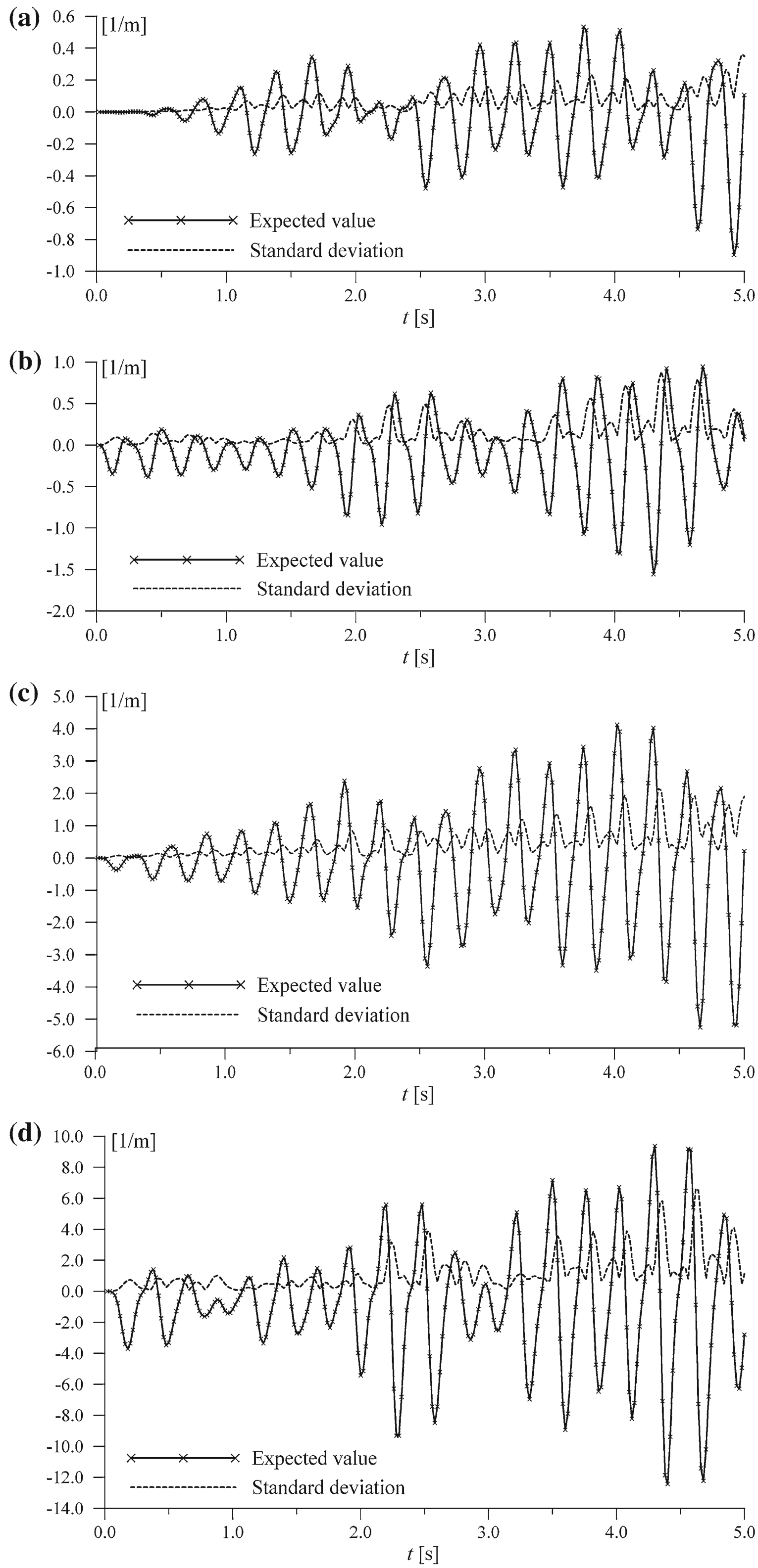

Fig. 10 Dynamic displacement sensitivity of: **a** el. No. 55, **b** el. No. 102, **c** el. No. 114, **d** el. No. 124—cross-sectional areas as a random design variables

Presented results prove that stochastic sensitivity analysis of dynamic systems may be important for design purposes. Randomness of design parameters reflects the reality, inaccuracies in construction, slight destruction of building elements. Time instant sensitivity analysis shows how the response of a system is dependent on design parameters and reveals negative dynamic phenomena, e.g., beat effect. Dynamic sensitivity results obtained in the stochastic context provide more information about the response of the system and allow us to specify the so-called design point.

In the discussed examples, damping effects were omitted. Selecting the appropriate damping factor even more reflects the real structural response. Taking into account damping effects is the problem of further analysis.

Acknowledgments Authoress wishes to thank Professor Tran Duong Hien for sharing the computer code POLSAP.

References

1. Zienkiewicz, O.C., Taylor, R.L.: The Finite Element Method, vol. 1. McGrew-Hill, London (1989)
2. Zienkiewicz, O.C., Taylor, R.L.: The Finite Element Method, vol. 2. McGrew-Hill, London (1993)
3. Bathe, K.-J.: Finite Element Procedures. Prentice-Hall, New Jersey (1996)
4. Haugh, E.J., Choi, K.K., Komkov, V.: Design Sensitivity Analysis of Structural Systems. Academic Pres, Orlando, FL (1986)
5. Mroz, Z., Haftka, R.T.: First- and second-order sensitivity analysis of linear and nonlinear systems. AIAA J. **24**, 1187–1192 (1986)
6. Mroz, Z., Bojczuk, D.: Shape and topology sensitivity analysis and its application to structural design. Arch. Appl. Mech. **82**, 1541–1555 (2012)
7. Bojczuk, D., Mroz, Z.: Topological sensitivity derivative with respect to area, shape and orientation of an elliptic hole in a plate. Struct. Multidisc. Optim. **45**, 153–169 (2012)
8. Choi, K.K., Kim, N.-H.: Structural Sensitivity Analysis and Optimization. Springer, New York (2010)
9. Drewko, J., Hien, T.D.: First- and second-order sensitivities of beams with respect to cross-sectional cracks. Arch. Appl. Mech. **74**, 309–324 (2005)
10. Ding, J., Pan, Z., Chen, L.: Parameter identification of multibody systems based on second order sensitivity analysis. Int. J. of Non-Linear Mech. **47**, 1105–1110 (2012)
11. Zona, A., Barbato, M., Conte, J.P.: Finite element response sensitivity analysis of continuous steel–concrete composite girders. Steel Compos. Struct. **6**(3), 183–202 (2006)
12. Billmaier, M., Bucher, C., Adam, C.: Selective sensitive finite element model updating: an improved approach. Struct. Contr. Health Monit. **21**, 1170–1192 (2014)
13. Ghanem, R.G., Spanos, P.D.: Stochastic Finite Elements: A Spectral Approach. Springer, New York (1991)
14. Hisada, T., Nakagiri, S.: Stochastic finite element method developed for structural safety and reliability. In: Proceedings of the 3rd International Conference on Structural Safety and Reliability, pp. 395–408. Trondheim (1981)
15. Liu, W.K., Belytschko, T., Mani, A.: Random field finite elements. Int. J. Numer. Methods Eng. **23**, 1831–1845 (1986)
16. Li, J., Chen, J.: Stochastic Dynamics of Structures. Wiley, Singapore (2009)
17. Greene, M.S., Liu, Y., Chen, W., Liu, W.K.: Computational uncertainty analysis in multiresolution materials via stochastic constitutive theory. Comput. Methods Appl. Mech. Eng. **200**, 309–325 (2011)
18. Kleiber, M., Hien, T.D.: The Stochastic Finite Element Method. Wiley, New Jersey (1992)
19. Kleiber, M., Hien, T.D.: Stochastic structural design sensitivity of static response. Int. J. Comput. Struct. **38**, 659–667 (1991). (Pergamon Press)
20. Sluzalec, A.: Stochastic shape sensitivity in powder metallurgy processing. Appl. Math. Model. **36**, 3743–3752 (2012)
21. Rahman, S.: Stochastic sensitivity analysis by dimensional decomposition and score functions. Probab. Eng. Mech. **24**, 278–287 (2009)
22. Jablonka, A., Hien, T.D.: A modified perturbation scheme for structural statics systems with random parameters. Arch. Appl. Mech. **84**, 821–831 (2014)
23. Jablonka, A., Hien, T.D.: Damping and dynamic sensitivity. Pomiary Automatyka Kontrola **57**, 1040–1043 (2011). (in Polish: Tlumienie a wrazliwosc dynamiczna)
24. Jablonka, A.: Numerical dynamic analysis of complex structures (in Polish: Numeryczna analiza dynamiczna konstrukcji zlozonych). Badania i analizy wybranych zagadnien z budownictwa. Praca zbiorowa pod red. Joanny Bzowki, pp. 535–543. Wydawnictwo Politechniki Slaskiej, Gliwice (2011)
25. Hien, T.D., Kleiber, M.: POLSAP—A Finite Element Code for Deterministic and Stochastic Analyses of Large 3D Structures. IPPT PAN, Warszawa (1990)
26. Wolfram, S.: The Mathematica Book, 4th edn. Cambridge University Press and Wolfram Media, Cambridge (2000)